ON THE SPECTRA OF CARBON NANO-STRUCTURES

PETER KUCHMENT AND OLAF POST

Abstract. An explicit derivation of dispersion relations and spectra for periodic Schrödinger operators on carbon nano-structures (including graphene and all types of single-wall nano-tubes) is provided.

1. Introduction

Carbon nano-structures, in particular fullerenes (buckyballs), carbon nanotubes, and graphene have attracted a lot of attention recently, due to their peculiar properties and existing or expected applications (e.g., [21, 25, 55]). Such structures have in particular been modelled by quantum networks (e.g., [2, 3, 26, 27]), also called quantum graphs, which goes back to quantum graph models in chemistry [51, 54] and physics [1, 5, 11, 48, 45] (see also [7, 32, 33] and references therein). A direct and inverse spectral study of Schrödinger operators on zig-zag carbon nano-tubes was conducted in [26, 27].

In this paper, we take a different from [26, 27] approach to such a study. Namely, we provide a simple explicit derivation of the dispersion relations for Schrödinger operators on the graphene structure, which in turn implies the structure of the spectrum and density of states. This derivation was triggered by the one done in [36] for the photonic crystal case, as well by [2, 3], albeit the presented computation is simpler and more convenient for our purpose than the one in [36]. It reflects the known idea (e.g., [1, 5, 34, 35, 50]) that spectral analysis of quantum graph Hamiltonians (at least on graphs with all edges of equal lengths) splits into two essentially unrelated parts: analysis on a single edge, and then spectral analysis on the combinatorial graph, the former being independent on the graph structure, and the latter independent on the potential.

The results are formulated in terms of the monodromy matrix (or rather its trace, also called the Hill discriminant [17]) of the $1D$ potential on one edge of the graphene lattice. Then this dispersion relation, just by simple restriction procedure, gives answers for any carbon nano-tube: zig-zag, armchair, or chiral. We would like to emphasize that relations of properties of the discriminant to the properties of the one-dimensional periodic potential have been studied for a long time and are understood by now extremely well (e.g., [12, 17, 18, 19, 24, 41, 43, 44, 53, 58] and references therein). Thus, one can extract all spectral information that might be needed, from our explicit description of dispersion relations that involve the discriminant.

Date: January 17, 2007.

2000 *Mathematics Subject Classification.* 92E10, 05C90, 58J50, 58J90, 81V99, 94C15.

Key words and phrases. carbon nano-tube, graphene, quantum graph, quantum network, spectrum, dispersion relation.

The paper is structured as follows: in the next Section 2, the main geometries and operators are introduced. Section 3 is devoted to derivation of the dispersion relation and the spectral structure for graphene, the main results provided in Theorem 3.6. The following Section 4 deals with nano-tubes. The main results accumulated in Theorem 4.3 provide dispersion relations and all parts of the spectra of the nano-tube operators. The last sections contain additional remarks and results, and acknowledgments.

2. Schrödinger operators on carbon nano-structures

All structures studied in this text can be introduced through the honeycomb graphene structure [21, 25, 55]. So, we start with discussing the latter.

2.1. **Graphen.** It is assumed that in graphene, the carbon atoms are situated at the vertices of a hexagonal $2D$ structure G shown in Fig. 1 below. We will

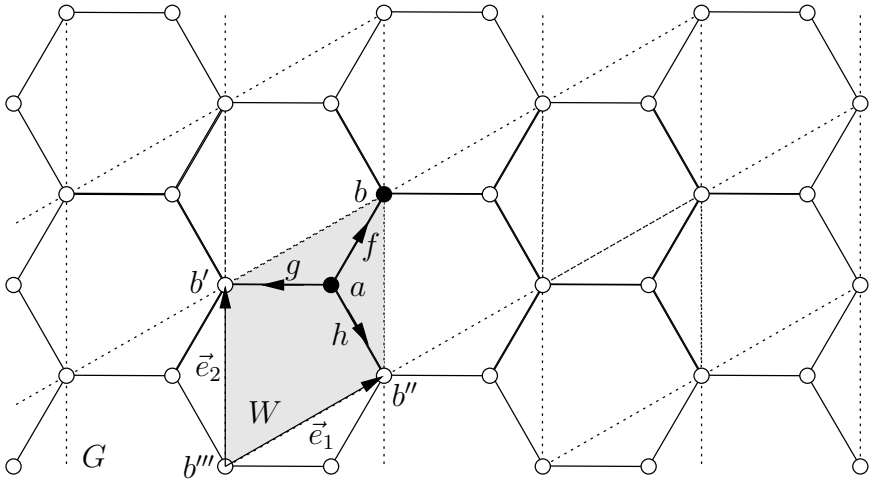

Figure 1. The hexagonal lattice G and a fundamental domain W together with its set of vertices $V(W) = \{a, b\}$ and set of edges $E(W) = \{f, g, h\}$.

assume that all edges of G have length 1. It will be crucial for us to consider the following action of the group $\mathbb{Z}^2$ on G: it acts by the shifts by vectors $p_1\vec{e}_1 + p_2\vec{e}_2$, where $(p_1, p_2) \in \mathbb{Z}^2$ and vectors $\vec{e}_1 = (3/2, \sqrt{3}/2)$, $\vec{e}_2 = (0, \sqrt{3})$ are shown in Fig. 1. We choose as a fundamental domain (Wigner-Seitz cell) of this action the parallelogram region W shown in the picture. Here two vertices $V(W) = \{a, b\}$ are assumed to belong to W, while the vertices b', b'' and b''' belong to other shifted copies of the fundamental domain. Three edges f, g, h belong to W. Although the graph G does not have to be directed, it will be convenient for us to assign directions to the edges in W as shown in the picture.

We will now equip the graph G with the structure of a quantum graph (quantum network) [7, 28, 29, 33, 34]. This requires introduction of a metric structure and of a differential Hamiltonian. We assume that G is naturally embedded into the Euclidean plane, which induces the arc length metric on G, as well as the identification of each edge e in G with the segment $[0, 1]$. Under this identification, the end points of an edge correspond to the points 0 and 1 (this identification

is unique up to a symmetry with respect to the center of the edge, i.e., up to the direction of the edge). We also obtain a measure (that we will call dx), and the ability to differentiate functions along edges and to integrate functions on G. In particular, the Hilbert space $L_2(G) := \bigoplus_{e\in E(G)} L_2(e)$ consisting of all square integrable functions on G can be naturally defined. Here $E(G)$ denotes the set of edges in G.

We now describe the graphene Hamiltonian H in $L_2(G)$ that will be studied in our paper (it has also been considered for some special potentials in [2]). Such operators are used for approximating the band structure of carbon nano-structures, as well of other compounds (e.g., [2, 3, 54], and references therein). Let $q_0(x)$ be an L_2-function on the segment $[0, 1]$. We will assume that it is even:

$$q_0(x) = q_0(1 - x). \tag{2.1}$$

The evenness assumption is made not just for mathematical convenience. As the proposition below shows, this condition is required if one considers operators invariant with respect to all symmetries of the graphene lattice. One could consider a directed honeycomb graph, and thus avoid the evenness condition (hence losing invariance of the operator), but the authors did not see any compelling physical reason for doing so.

Using the fixed identification of the edges $e \in E(G)$ with $[0, 1]$, we can pullback the function $q_0(x)$ to a function (*potential*) $q(x)$ on G. Notice, that due to the evenness condition imposed on $q_0(x)$, the definition of the potential q does not depend on the orientations chosen along the edges. It is also easy to see that the following claim holds:

Proposition 2.1. *The potential q defined as above, is invariant with respect to the full symmetry group of the honeycomb lattice G. Moreover, all invariant potentials from $L_{2,\mathrm{loc}}(G)$ are obtainable by this procedure.*

We skip the immediate proof of this statement.

We can now define our Hamiltonian H. It acts along each edge e as

$$Hu(x) = -\frac{d^2u(x)}{dx^2} + q(x)u(x), \tag{2.2}$$

where we use the shorthand notation x for the coordinate x_e along the edge e.

The domain $\operatorname{dom} H$ of the operator H consists of the functions u that belong to the Sobolev space $H^2(e)$ on each edge e in G and satisfy the inequality

$$\sum_{e\in E(G)} \|u\|^2_{H^2(e)} < \infty. \tag{2.3}$$

They also must satisfy the so-called *Neumann vertex conditions* (also somewhat misleadingly called *Kirchhoff vertex conditions*) at vertices. These conditions require continuity of the functions at each vertex v (and thus on all graph G) and vanishing of the total flux, i.e.,

$$u_{e_1}(v) = u_{e_2}(v) \qquad \text{if } e_1, e_2 \in E_v(G), \tag{2.4a}$$

$$\sum_{e\in E_v(G)} u'_e(v) = 0 \tag{2.4b}$$

at each vertex $v \in V(G)$. Here $E_v(G) := \{ e \in E(G) \,|\, v \in e \}$ is the set of edges adjacent to the vertex v, u_e is the restriction of a function u to the edge e, and $u'_e(v)$ denotes the derivative of u_e along e in the direction away from the vertex v (*outgoing direction*). Thus defined operator H is unbounded and self-adjoint in the Hilbert space $L_2(G)$ [28, 34]. Due to the condition on the potential and Proposition 2.1, the Hamiltonian H is invariant with respect to all symmetries of the hexagonal lattice G, in particular with respect to the $\mathbb{Z}^2$-shifts, which will play a crucial role in our considerations.

2.2. **Nano-tubes.** We provide here a very brief introduction to carbon nano-tubes. One can find more detailed discussion and classification of nano-tubes in [21, 55]. We also emphasize that only single-wall nano-tubes are considered.

Let $p \in \mathbb{R}^2 \backslash \{\vec{0}\}$ be a vector that belongs to the lattice of translation symmetries of the honeycomb structure G. In other words, $G + p = G$. Let us denote by ι_p the equivalence relation that identifies vectors $z_1, z_2 \in G$ such that $z_2 - z_1$ is an integer multiple of the vector p. A *nano-tube* T_p is the graph obtained as the quotient of G with respect to this equivalence relation:

$$T_p := G/\iota_p. \tag{2.5}$$

This graph is naturally isometrically embedded into the cylinder $\mathbb{R}^2/\iota_p$.

If $p = p_1\vec{e}_1 + p_2\vec{e}_2$, we will abuse notations denoting T_p by $T_{(p_1,p_2)}$. For example, $T_{(0,N)}$ is the so-called *zig-zag nano-tube*, while $T_{(N,N)}$ is the so-called *armchair nano-tube*. The names come from the shape of the boundary of a fundamental domain (cf. Fig. 2). There are many other types of nano-tubes, besides the zig-zag

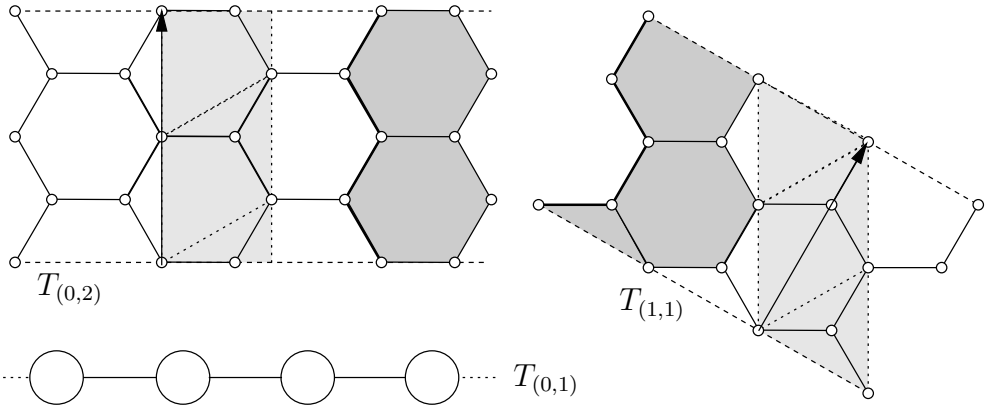

FIGURE 2. A *zig-zag* (left) and *armchair* (right) nano-tube $T_{(0,2)}$ and $T_{(1,1)}$, respectively. The vectors show the translation vector p. The name-giving fundamental domain of each of the nano-tubes is shaded in dark grey. The dashed lines have to be identified. Below, the (degenerate) zig-zag nano-tube $T_{(0,1)}$ is shown.

and armchair ones. They are usually called *chiral*.

A degenerate example is given by the zig-zag nano-tube $T_{(0,1)}$, which consists of a sequence of loops ("beads") joined by edges into a $1D$-periodic *necklace structure* (see Fig. 2).

One can notice that due to existence of rotational and mirror symmetries of the hexagonal structure G, different vectors p can produce the same nano-tubes T_p. For instance, $T_{(m,n)} = T_{(n,m)}$. Also, zig-zag tubes $T_{(0,N)}, T_{(N,0)}$, and $T_{(N,-N)}$ are the same (see [21] and references therein for a more detailed classification of nano-tubes).

The Hamiltonian H_p on $T = T_p$ is defined exactly as for the graphene lattice G. Alternatively, one can think of H acting on functions on G that are periodic with the period vector p (this definition requires some precision, since such functions do not belong to $L_2(G)$).

3. Spectra of graphene operators

Here we calculate the dispersion relation and thus all parts of the spectrum of the graphene Hamiltonian H (see also [2, 3] for related considerations). One can notice that the density of states is determined by the dispersion relation, and thus when the latter is known, the former can be determined as well [4, 53].

We apply now the standard Floquet-Bloch theory (e.g., [17, 31, 53]) with respect to the $\mathbb{Z}^2$-action that we specified before. This theory also holds in the quantum graph case, (see, e.g., [14, 15, 30, 35, 49] and references therein). This reduces the study of the Hamiltonian H to the study of the family of Bloch Hamiltonians H^θ acting in $L_2(W)$ for the values of the *quasimomentum* θ in the Brillouin zone $[-\pi, \pi]^2$. Here the Bloch Hamiltonian H^θ acts the same way H does, but it is applied to a different space of functions. Each function $u = \{u_e\}$ in the domain of H^θ must belong to the Sobolev space $u_e \in H^2(e)$ on each edge e and satisfy the vertex conditions (2.4), as well as the *cyclic conditions* (Floquet-Bloch conditions)

$$u(x + p_1\vec{e}_1 + p_2\vec{e}_2) = \mathrm{e}^{\mathrm{i}p\cdot\theta}u(x) = \mathrm{e}^{\mathrm{i}(p_1\theta_1 + p_2\theta_2)}u(x) \tag{3.1}$$

for any vector $p = (p_1, p_2) \in \mathbb{Z}^2$ and any $x \in G$.

Due to the conditions (3.1), functions u are uniquely determined by their restrictions to the fundamental domain W. Then conditions (2.4) and (3.1) reduce to

$$\begin{cases} u_f(0) = u_g(0) = u_h(0) =: A \\ u'_f(0) + u'_g(0) + u'_h(0) = 0 \\ u_f(1) = \mathrm{e}^{\mathrm{i}\theta_1}u_g(1) = \mathrm{e}^{\mathrm{i}\theta_2}u_h(1) =: B \\ u'_f(1) + \mathrm{e}^{\mathrm{i}\theta_1}u'_g(1) + \mathrm{e}^{\mathrm{i}\theta_1}u'_h(1) = 0. \end{cases} . \tag{3.2}$$

By standard arguments (see e.g. [34, Theorem 18]), H^θ has purely discrete spectrum $\sigma(H^\theta) = \{\lambda_j(\theta)\}$. The graph of the multiple valued function $\theta \mapsto \{\lambda_j(\theta)\}$ is known as the *dispersion relation*, or *Bloch variety* of the operator H. It is known [17, 24, 31, 53] that the range of this function is the spectrum of H:

$$\sigma(H) = \bigcup_{\theta\in[-\pi,\pi]^2} \sigma(H^\theta). \tag{3.3}$$

It is also well known that the dispersion relation determines not only the spectrum, but the density of states of H as well [4, 53].

So, our goal now is the determination of the spectrum of H^θ and thus the dispersion relation of H. In order to determine this spectrum, we have to solve

the eigenvalue problem

$$H^\theta u = \lambda u \tag{3.4}$$

for $\lambda \in \mathbb{R}$ and a non-trivial function $u \in L_2(W)$ satisfying the above boundary conditions.

Let us denote by Σ^{D} the spectrum of the Dirichlet Hamiltonian H^{D} acting as in (2.2) on $(0,1)$ with boundary conditions $u(0) = u(1) = 0$. If $\lambda \notin \Sigma^{\mathrm{D}}$, there exist two linearly independent solutions φ_0, φ_1 (depending on λ) of the equation

$$-\varphi'' + q_0\varphi = \lambda\varphi \tag{3.5}$$

on $(0,1)$, such that $\varphi_0(0) = 1$, $\varphi_0(1) = 0$ and $\varphi_1(0) = 0$, $\varphi_1(1) = 1$. For example, if $q_0 = 0$ and $\lambda > 0$ then we have $\lambda \notin \Sigma^{\mathrm{D}}$ if and only if $\mu := \sqrt{\lambda} \notin \pi\mathbb{Z}$ and

$$\varphi_0(t) = \frac{\sin\mu(1-t)}{\sin\mu} \qquad \text{and} \qquad \varphi_1(t) = \frac{\sin\mu t}{\sin\mu}. \tag{3.6}$$

We will often use the notation $\varphi_{0,\lambda}, \varphi_{1,\lambda}$ to emphasize dependence on the spectral parameter.

We will assume that the functions φ_j are lifted to each of the edges in W, using the described before identifications of these edges with the segment $[0,1]$. Abusing notations, we will use the same names φ_j for the lifted functions. Then, for $\lambda \notin \Sigma^{\mathrm{D}}$ we can use (3.2) to represent any solution u of (3.4) from the domain of H^θ on each edge in W as follows:

$$\begin{cases} u_f = A\varphi_0 + B\varphi_1 \\ u_g = A\varphi_0 + \mathrm{e}^{-\mathrm{i}\theta_1}B\varphi_1 \\ u_h = A\varphi_0 + \mathrm{e}^{-\mathrm{i}\theta_2}B\varphi_1. \end{cases} \tag{3.7}$$

With this choice, the continuity conditions in (3.2) and the eigenvalue equation on each edge are automatically satisfied. The remaining two equations that guarantee zero fluxes at the vertices, lead to the system

$$\begin{cases} 3\varphi_0'(0)A + (1 + \mathrm{e}^{-\mathrm{i}\theta_1} + \mathrm{e}^{-\mathrm{i}\theta_2})\varphi_1'(0)B = 0 \\ (1 + \mathrm{e}^{\mathrm{i}\theta_1} + \mathrm{e}^{\mathrm{i}\theta_2})\varphi_0'(1)A + 3\varphi_1'(1)B = 0. \end{cases} \tag{3.8}$$

Using the symmetry (2.1) of the potential q_0, we obtain

$$\varphi_1'(1) = -\varphi_0'(0) \qquad \text{and} \qquad \varphi_0'(1) = -\varphi_1'(0). \tag{3.9}$$

Thus, the system (3.8) reduces to

$$\begin{cases} -3\varphi_1'(1)A + (1 + \mathrm{e}^{-\mathrm{i}\theta_1} + \mathrm{e}^{-\mathrm{i}\theta_2})\varphi_1'(0)B = 0 \\ (1 + \mathrm{e}^{\mathrm{i}\theta_1} + \mathrm{e}^{\mathrm{i}\theta_2})\varphi_1'(0)A - 3\varphi_1'(1)B = 0. \end{cases} \tag{3.10}$$

The quotient

$$\eta(\lambda) := \frac{\varphi_1'(1)}{\varphi_1'(0)} = \frac{\varphi_{1,\lambda}'(1)}{\varphi_{1,\lambda}'(0)} \tag{3.11}$$

is well defined, since $\varphi_1'(0) \neq 0$. Thus, the system (3.10) can be rewritten as

$$\begin{cases} -3\eta(\lambda)A + (1 + \mathrm{e}^{-\mathrm{i}\theta_1} + \mathrm{e}^{-\mathrm{i}\theta_2})B = 0 \\ (1 + \mathrm{e}^{\mathrm{i}\theta_1} + \mathrm{e}^{\mathrm{i}\theta_2})A - 3\eta(\lambda)B = 0. \end{cases} \tag{3.12}$$

The determinant of this system is clearly equal to

$$\begin{aligned} &|1+\mathrm{e}^{\mathrm{i}\theta_1}+\mathrm{e}^{\mathrm{i}\theta_2}|^2-9\eta^2(\lambda)\\ &=3+2\cos\theta_1+2\cos\theta_2+2\cos(\theta_1-\theta_2)-9\eta^2(\lambda)\\ &=1+8\cos\tfrac{\theta_1-\theta_2}{2}\cos\tfrac{\theta_1}{2}\cos\tfrac{\theta_2}{2}-9\eta^2(\lambda). \end{aligned} \tag{3.13}$$

Thus, we have proven the following lemma:

Lemma 3.1. *If $\lambda\notin\Sigma^{\mathrm{D}}$, then λ is in the spectrum of the graphene Hamiltonian H if and only if there is $\theta\in[-\pi,\pi]^2$ such that*

$$9\eta^2(\lambda)=|1+\mathrm{e}^{\mathrm{i}\theta_1}+\mathrm{e}^{\mathrm{i}\theta_2}|^2,$$

or

$$9\eta^2(\lambda)=1+8\cos\frac{\theta_1-\theta_2}{2}\cos\frac{\theta_1}{2}\cos\frac{\theta_2}{2}. \tag{3.14}$$

Remark 3.2. Note that this lemma gives a nice relation between the spectrum of the metric graph Hamiltonian H and the discrete graph Laplacian [9, 10] $\Delta U:=\frac{1}{\deg v}\sum_{w\sim v}U(w)$. Indeed, the Bloch Laplacian Δ^θ on $\ell_2(\{a,b\})\cong\mathbb{C}^2$ has the matrix

$$\Delta^\theta\cong\frac{1}{3}\begin{pmatrix}0 & 1+\mathrm{e}^{-\mathrm{i}\theta_1}+\mathrm{e}^{-\mathrm{i}\theta_2}\\ 1+\mathrm{e}^{\mathrm{i}\theta_1}+\mathrm{e}^{\mathrm{i}\theta_2} & 0\end{pmatrix}.$$

Thus, the lemma is just the statement that for $\lambda\notin\Sigma^{\mathrm{D}}$, we have $\lambda\in\sigma(H^\theta)$ if and only if $\eta(\lambda)\in\sigma(\Delta^\theta)$, and hence $\lambda\in\sigma(H)$ if and only if $\eta(\lambda)\in\sigma(\Delta)$.

This relation between quantum and combinatorial graph operators is well known and has been exploited many times (e.g., [1, 5, 8, 34, 35, 39, 50]).

Lemma 3.1, in particular, says that in order to find the spectrum of H, we need to calculate the range of the following function on $[-\pi,\pi]^2$:

$$F(\theta_1,\theta_2)=\sqrt{1+8\cos\frac{\theta_1-\theta_2}{2}\cos\frac{\theta_1}{2}\cos\frac{\theta_2}{2}}. \tag{3.15}$$

Lemma 3.3. *The function F has range $[0,3]$; its maximum is attained at $(0,0)$ and minimum at $(2\pi/3,-2\pi/3)$ and $(-2\pi/3,2\pi/3)$.*

The proof of the lemma is straightforward, after noticing that the function

$$F(\theta_1,\theta_2)^2=1+8\cos\frac{\theta_1-\theta_2}{2}\cos\frac{\theta_1}{2}\cos\frac{\theta_2}{2}=|1+\mathrm{e}^{\mathrm{i}\theta_1}+\mathrm{e}^{\mathrm{i}\theta_2}|^2$$

ranges from 0 to 9.

Next, we want to interpret the function $\eta(\lambda)$ in terms of the original potential $q_0(x)$ on $[0,1]$. To this end, let us extend $q_0(x)$ periodically to the whole real axis $\mathbb{R}$ and consider the Hill operator H^{per} on $\mathbb{R}$ given as in (2.2) with the resulting periodic potential:

$$H^{\mathrm{per}}u(x)=-\frac{d^2u(x)}{dx^2}+q_0(x)u(x). \tag{3.16}$$

(We maintain the notation $q_0(x)$ for the extended potential.)

We will be interested in the well studied spectral problem

$$H^{\mathrm{per}}u=\lambda u \tag{3.17}$$

As it is usually done in the theory of periodic Hill operators (e.g., [17, 24, 41, 12, 53]), we consider the so called *monodromy matrix* $M(\lambda)$ of H^{per}. It is defined as follows:

$$\begin{pmatrix} \varphi(1) \\ \varphi'(1) \end{pmatrix} = M(\lambda) \begin{pmatrix} \varphi(0) \\ \varphi'(0) \end{pmatrix}$$

where φ is any solution of (3.17). In other words, the monodromy matrix shifts by the period along the solutions of (3.17). The matrix valued function $\lambda \mapsto M(\lambda)$ is entire.

It is well known (see the references above) and easy to see that the monodromy matrix has determinant equal to 1. Its trace plays the major role in the spectral theory of the Hill operator. Namely, let $D(\lambda) = \operatorname{tr} M(\lambda)$ be the so called *discriminant* (or Lyapunov function) of the Hill operator H^{per}. The next proposition collects well known results concerning the spectra of Hill operators [17, 24, 41, 12, 53]:

Proposition 3.4.

(i) *The spectrum $\sigma(H^{\mathrm{per}})$ of H^{per} is purely absolutely continuous.*

(ii) $\sigma(H^{\mathrm{per}}) = \left\{ \lambda \in \mathbb{R} \,\middle|\, |D(\lambda)| \le 2 \right\}$.

(iii) *$\sigma(H^{\mathrm{per}})$ consists of the union of closed non-overlapping and non-zero lengths finite intervals* (bands) $B_{2k} := [a_{2k}, b_{2k}]$, $B_{2k+1} := [b_{2k+1}, a_{2k+1}]$ *such that*

$$a_0 < b_0 \le b_1 < a_1 \le a_2 < b_2 \le \dots$$

and $\lim_{k\to\infty} a_k = \infty$.

The (possibly empty) segments (b_{2k}, b_{2k+1}) and (a_{2k+1}, a_{2k+2}) are called the spectral gaps.

Here $\{a_k\}$ and $\{b_k\}$ are the spectra of the operator with periodic and anti-periodic conditions on $[0,1]$ correspondingly.

(iv) *Let $\lambda_k^{\mathrm{D}} \in \Sigma^{\mathrm{D}}$ be the kth Dirichlet eigenvalue, labelled in increasing order. Then λ_k^{D} belongs to (the closure of) the kth gap*[1]*. When q_0 is symmetric, as in our case, λ_k^{D} coincides with an edge of the kth gap*[2]*.*

(v) *If λ is inside the kth band B_k, then $D'(\lambda) \neq 0$, and $D(\lambda)$ is a homeomorphism of the band B_k onto $[-2,2]$. Moreover, $D(\lambda)$ is decaying on $(-\infty, b_0)$ and (a_{2k}, b_{2k}) and is increasing on (b_{2k+1}, a_{2k+1}). It has a simple extremum in each spectral gap $[a_k, a_{k+1}]$ and $[b_k, b_{k+1}]$.*

(vi) *The dispersion relation for H^{per} is given by*

$$D(\lambda) = 2\cos\theta, \tag{3.18}$$

where θ is the one-dimensional quasimomentum.

There are many other important direct and inverse spectral results concerning the well studied (in particular, due to the inverse scattering transform research) operator H^{per} (see, e.g., [17, 18, 19, 24, 44, 41, 43, 53, 58]).

We will now see the relation between the function $\eta(\lambda)$ that was introduced for the graphene operator H and the discriminant of H^{per}. In order to do so, we introduce another basis of solutions of (3.17), namely c_λ and s_λ with $c_\lambda(0) = 1$,

[1] If the gap closes, this boils down to a single point.

[2] The same comment applies here.

$c'_\lambda(0) = 0$ and $s_\lambda(0) = 0$, $s'_\lambda(0) = 1$ (the notations are chosen to remind the cosine and sine functions in the case of zero potential). Using this basis of the solution space, we obtain

$$M(\lambda) = \begin{pmatrix} c_\lambda(1) & s_\lambda(1) \\ c'_\lambda(1) & s'_\lambda(1) \end{pmatrix}. \tag{3.19}$$

A simple calculation (assuming the symmetry (2.1)) relates the new basis with the one of φ_0 and φ_1 (which we now denote $\varphi_{0,\lambda}, \varphi_{1,\lambda}$ to emphasize dependence on the spectral parameter):

$$c_\lambda = \varphi_{0,\lambda} + \eta(\lambda)\varphi_{1,\lambda} \qquad \text{and} \qquad s_\lambda = \frac{1}{\varphi'_{1,\lambda}(0)}\varphi_{1,\lambda}.$$

In particular, $c_\lambda(1) = s'_\lambda(1) = \eta(\lambda)$. Thus,

$$\eta(\lambda) = \frac{1}{2}D(\lambda). \tag{3.20}$$

For example, if $q_0 = 0$, then $\eta(\lambda) = \cos(\sqrt{\lambda})$.

So far, we have been avoiding points of the Dirichlet spectrum Σ^{D} of a single edge (i.e, the Dirichlet spectrum of the potential $q_0(x)$ on $[0, 1]$). We will now deal with exactly these points.

Lemma 3.5. *Each point $\lambda \in \Sigma^{\mathrm{D}}$ is an eigenvalue of infinite multiplicity of the graphene Hamiltonian H. The corresponding eigenspace is generated by simple loop states, i.e., by eigenfunctions which live on a single hexagon and vanish at the vertices (see Fig. 3 below).*

Proof. We need to guarantee first that each $\lambda \in \Sigma^{\mathrm{D}}$ is an eigenvalue. Indeed, an eigenfunction is provided by a simple loop state of the type shown for zero potential in Fig. 3 below. It is constructed as follows. Let $\psi_\lambda(x)$ be an eigenfunction

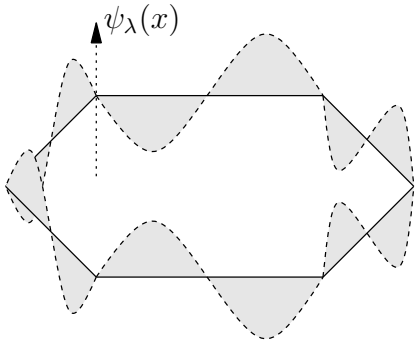

FIGURE 3. A simple loop state constructed from an odd eigenfunction on $[0, 1]$.

of the operator $-d^2/dx^2 + q_0(x)$ with the eigenvalue λ and Dirichlet boundary conditions on $[0, 1]$. Then, due to the symmetry (evenness) of the potential, we can assume the eigenfunction to be either even, or odd. For an odd eigenfunction $\psi_\lambda(x)$, repeating it on each of the six edges of a hexagon, we clearly get

an eigenfunction of the operator H. If it is an even eigenfunction, then repeating it around the hexagon with an alternating sign does the same trick. Thus $\lambda \in \sigma_{\rm pp}(H)$.

It is well known then (e.g., [17]) that the multiplicity of the eigenvalue must be infinite. For completeness, we repeat here this simple argument. Let $M_\lambda \subset L_2(G)$ be the eigenspace. Consider a vector γ that is a period of the lattice G and the operator S_γ of shift by γ in $L_2(G)$. Then S_γ acts in M_λ as a unitary operator. If $\dim M_\lambda$ were finite, S_γ would have had an eigenvector $f \in M_\lambda \subset L_2(G)$ with an eigenvalue μ, $|\mu| = 1$. However, such a function f obviously cannot belong to $L_2(G)$, since it is quasi-periodic in the direction of the vector γ. This proves infinite multiplicity.

We note now that due to [30] (see also [35, Thm. 11]), linear combinations of compactly supported eigenfunctions are dense in the whole eigenspace M_λ. Thus, we only need to show that the simple loop states just described generate all compactly supported eigenfunctions in the space M_λ.

Suppose that φ is a compactly supported eigenfunction of H corresponding to the eigenvalue $\lambda \in \Sigma^{\rm D}$. First, note that φ vanishes at each vertex. Indeed, if this were not true, due to compactness of support, there would have been an edge such that at its one end v_0 (corresponding to $x = 0$), $\varphi(v_0) \neq 0$, while at the other v_1 (corresponding to $x = 1$), $\varphi(v_1) = 0$. Expanding into the basis c_λ, s_λ, we get

$$\varphi(x) = Ac_\lambda(x) + Bs_\lambda(x).$$

In particular, $\varphi(0) = A \neq 0$. Then $\varphi(1) = Ac_\lambda(1) = As'_\lambda(1) \neq 0$, since $s_\lambda(1) = 0$. This leads to a contradiction. Thus, φ vanishes at all vertices. In particular, on each edge it constitutes a Dirichlet eigenfunction for the Hill operator on this edge.

This also implies that the support of φ, as a graph, cannot have vertices of degree 1 and $\operatorname{supp}\varphi$ cannot be a tree. Thus, there must be a loop in the support of φ. In particular, the outer boundary of the support must be a loop. Take one boundary edge e_0. There is a hexagon inside the boundary loop which contains this edge. Consider a simple loop state φ_0 coinciding with the eigenfunction φ on e_0 and extended to the hexagon the way it was described before. Subtracting φ_0 from φ, we obtain a new eigenfunction $\widetilde{\varphi}$. The number of hexagons inside the boundary loop of the support of $\widetilde{\varphi}$ is less than inside the support of φ. Thus, continuing this procedure, we eventually represent φ as a combination of simple loop eigenstates. Fig. 4 below illustrates this process. □

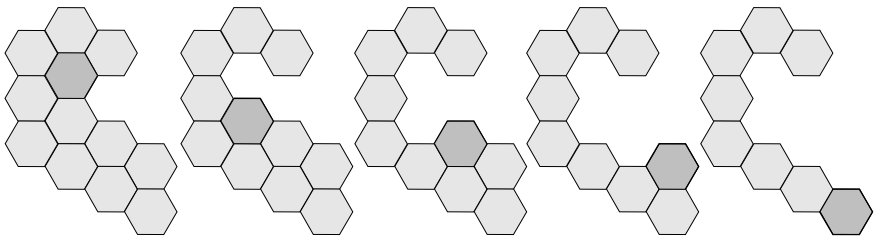

FIGURE 4. Deleting simple loop states (dark grey) from the support of an eigenfunction (light grey).

We can now completely describe the spectral structure of the graphene operator H.

Theorem 3.6.

(i) *The singular continuous spectrum $\sigma_{\rm sc}(H)$ is empty.*

(ii) *The absolutely continuous spectrum $\sigma_{\rm ac}(H)$ has band-gap structure and coincides as a set with the spectrum $\sigma(H^{\rm per})$ of the Hill operator $H^{\rm per}$ with potential q_0 periodically extended from $[0,1]$. In particular,*

$$\sigma_{\rm ac}(H) = \big\{\, \lambda \in \mathbb{R} \,\big|\, |D(\lambda)| \le 2 \,\big\},$$

where $D(\lambda)$ is the discriminant of $H^{\rm per}$.

(iii) *The pure point spectrum $\sigma_{\rm pp}(H)$ coincides with $\Sigma^{\rm D}$ and thus, due to the evenness of the potential, belongs to the union of the edges of spectral gaps of $\sigma(H^{\rm per}) = \sigma_{\rm ac}(H)$.*

(iv) *The dispersion relation consists of the variety*

$$D(\lambda) = \pm\frac{2}{3}\sqrt{1 + 8\cos\frac{\theta_1-\theta_2}{2}\cos\frac{\theta_1}{2}\cos\frac{\theta_2}{2}} \tag{3.21}$$

and the collection of flat branches $\lambda \in \Sigma^{\rm D}$.

(v) *Eigenvalues $\lambda \in \Sigma^{\rm D}$ of the pure point spectrum are of infinite multiplicity and the corresponding eigenspaces are generated by simple loop eigenstates.*

In particular, $\sigma(H)$ has gaps if and only if $\sigma(H^{\rm per})$ has gaps.

Proof.

The claim (i) about absence of the singular continuous spectrum is a general fact about periodic "elliptic" operators. For instance, the standard proof applied for the case of periodic Schrödinger operators in [53, 56] or [31, Theorem 4.5.9] works in our situation. Alternatively, in [20] one can find this statement proven for a general case of *analytically fibered operators*, which covers our situation as well.

Statement (iv) is a combination of Lemmas 3.1 and 3.5 and formula (3.20).

The statement (ii) about absolute continuity of the spectrum outside the points of $\Sigma^{\rm D}$ follows from (iv) and the standard Thomas' analytic continuation argument [31, 53, 56]. We remind the reader that according to this argument, eigenvalues correspond to constant branches of the dispersion relation. It is clear that the dispersion curves (3.21) have no constant branches outside $\Sigma^{\rm D}$.

The claim (iii) is just a combination of Lemma 3.5 and of the Thomas' argument again, which shows that there are no eigenvalues outside $\Sigma^{\rm D}$.

Finally, (v) is a combination of (iii) and Lemma 3.5. □

It is clear that the function F^2 has non-degenerate minima $F = 0$ at the points $\theta = \pm(2\pi/3, -2\pi/3)$. Thus, the function $\pm F$ has conical singularities at these points. Since, according to Proposition 3.4, the discriminant D is monotonic with non-degenerate derivative near each point where $D(\lambda) = 0$, one obtains the following conclusion:

Corollary 3.7. *The dispersion curve of the graphene operator H has conical singularities at all spectral values λ such that $D(\lambda) = 0$.*

These singularities (sometimes described as "linear spectra") represent one of the most interesting features of graphene structures (cf. Fig. 5). These singu-

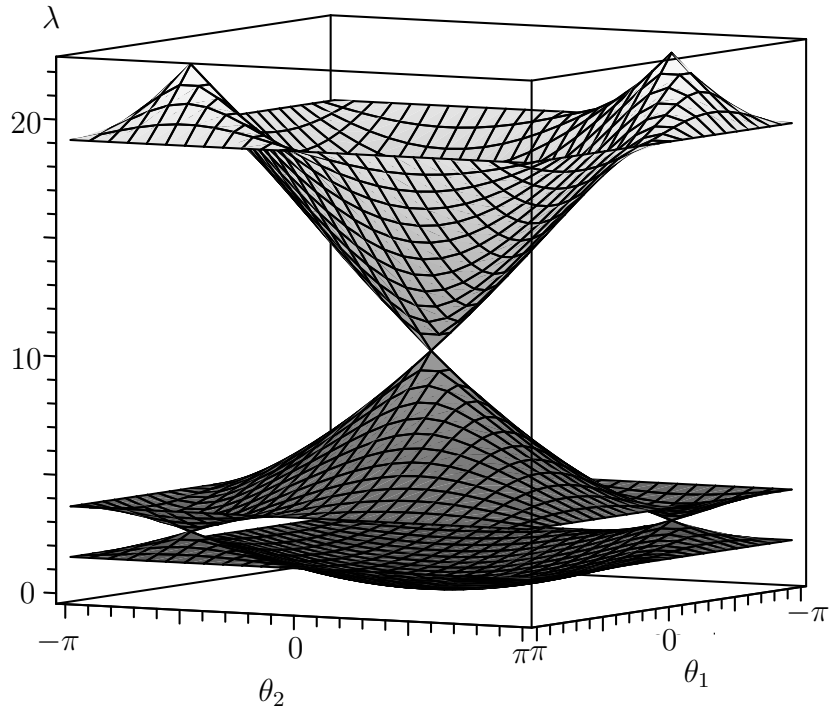

FIGURE 5. The dispersion relation $\cos\sqrt{\lambda} = \pm F(\theta)/3$ for the free (i.e., $q_0 = 0$) case. The cones arising from $D(\lambda) = 2\cos(\sqrt{\lambda}) = 0$ are at the levels $\lambda = (\pi(2k+1))^2$. They are located *inside* a band of the corresponding Hill operator. Note that the cones at $D(\lambda) = \pm 2$ (i.e., $\lambda = (\pi k)^2$ in the free case) are located at the *band edges* of the Hill operator.

larities resemble Dirac spectra for massless fermions and thus lead to unusual physical properties of graphene (e.g., [25]). We see that quantum graph models with arbitrary periodic potentials preserve this feature.

4. Spectra of nano-tube operators

We use here the notations concerning nano-tubes that were introduced in Section 2.2. Consider a vector $p = (p_1, p_2) \in \mathbb{Z}^2$ that belongs to the lattice of translation symmetries of the graphene structure G, i.e., it shifts the structure by $p_1\vec{e}_1 + p_2\vec{e}_2$ (see Fig. 1). We will use, as before, the corresponding nano-tube $T_p = T_{(p_1,p_2)}$ and the Hamiltonian $H_p = H_{(p_1,p_2)}$ on T_p (see Section 2.2).

Let $B = [-\pi, \pi]^2$ be the Brillouin zone of graphene. Then, as we discussed in the previous section, the Floquet-Bloch theory provides the direct integral

expansion

$$H = \int_B^{\oplus} H^\theta d\theta. \tag{4.1}$$

In the case of the nano-tube T_p, only the values of quasimomenta θ enter that satisfy the condition

$$p \cdot \theta = p_1\theta_1 + p_2\theta_2 \in 2\pi\mathbb{Z} \tag{4.2}$$

since a function on T_p lifts to a p-periodic function u on G, i.e.,

$$u(x + p_1\vec{e}_1 + p_2\vec{e}_2) = u(x)$$

(cf. (3.1)). Thus, let us consider the following subset $B_p \subset B$:

$$B_p := \big\{\, \theta \in [-\pi, \pi]^2 \,\big|\, p \cdot \theta \in 2\pi\mathbb{Z} \,\big\}. \tag{4.3}$$

Then, we have the direct integral decomposition

$$H_p = \int_{B_p}^{\oplus} H^\theta d\theta. \tag{4.4}$$

In particular, the spectrum of H_p is given by

$$\sigma(H_p) = \bigcup_{\theta \in B_p} \sigma(H^\theta), \tag{4.5}$$

and the dispersion relation for H_p is just the restriction to B_p of the dispersion relation for H described in the part (iv) of Theorem 3.6.

This implies for instance that we still have $\Sigma^{\mathrm{D}} \subset \sigma_{\mathrm{pp}}(H_p)$ and the rest of the spectrum is determined by the pre-image

$$\eta^{-1}\Big\{\pm\frac{1}{3}F(B_p)\Big\} = D^{-1}\Big\{\pm\frac{2}{3}F(B_p)\Big\}. \tag{4.6}$$

One should notice that it is conceivable that non-constant branches of the dispersion curves (3.14) might sometimes have constant restrictions to B_p, thus providing new eigenvalues for the nano-tube Hamiltonian. This happens if the line (4.2) is a level set of the function F. It is easy to find such lines.

Lemma 4.1. *The only linear level sets of the function F inside B are the following ones:*

(i) $\theta_1 = \pm\pi$
(ii) $\theta_2 = \pm\pi$
(iii) $\theta_1 - \theta_2 = \pm\pi$

On these lines $F(\theta_1, \theta_2) = 1$.

The proof of the lemma is immediate from the expression (3.15) for the function F (see also Fig. 6 for the level sets of F, which illustrates this statement). We will see that existence of such lines leads to additional pure point spectrum for some types of nano-tubes.

In order to determine the spectra of nano-tubes, we need to know the ranges of the function F (cf. (3.15)) restricted to B_p. These are described in the following

Lemma 4.2.

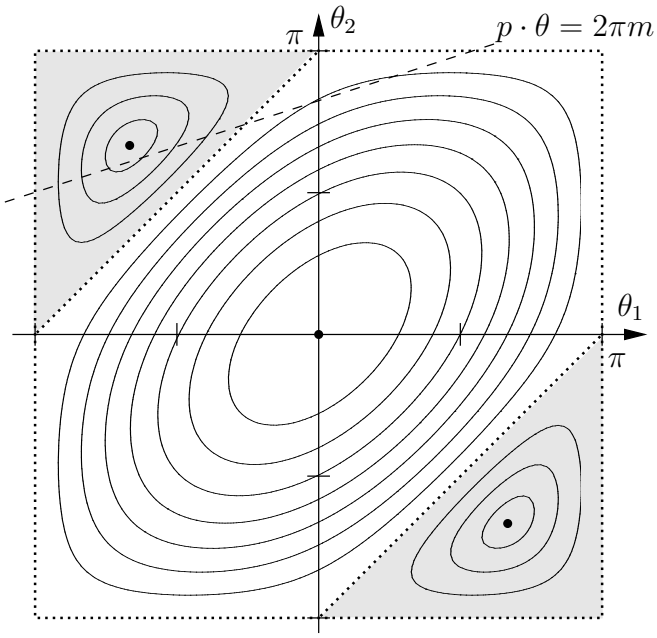

FIGURE 6. The level curves of F for levels varying from 0 (the two dots at $\pm(2\pi/3, -2\pi/3)$) till 3 (the dot at the origin). The level curve associated to $F = 1$ is dotted, the areas where $F < 1$ are shaded. The dashed line is the line in B_p closest to the minimum point $(-2\pi/3, 2\pi/3)$ (in the case $p_1 - p_2 = 3m \pm 1$).

(i) *The function F restricted to B_p, achieves its maximum 3 at $(0,0) \in B_p$ for any p.*

(ii) *The location and value of the minimum depends on the vector p. The minimal value*

$$\alpha(p) := \min_{\theta \in B_p} F(\theta)$$

satisfies

$$\alpha(p) \in [0, 1] \tag{4.7}$$

for any p.

(iii) *$\alpha(p) = 0$ if and only if $p_1 - p_2$ is divisible by 3.*

(iv) *$\alpha(p) = 1$ if and only if $p = (0, \pm 1)$, $(\pm 1, 0)$, $(0, \pm 2)$, $(\pm 2, 0)$, $(1, -1)$, $(-1, 1)$, $(2, -2)$, or $(-2, 2)$. (All these cases correspond to zig-zag nanotubes).*

(v) *In all cases not covered by (iii) and (iv), let $p_1 - p_2 = 3m \pm 1$. Then $\alpha(p) \in (0, 1)$ can be found by minimizing the function F over the line $p_1\theta_1 + p_2\theta_2 = 2\pi m$.*

In particular, in the case when $p = (0, N)$ with $N = 3m \pm 1 > 2$ ($m \in \mathbb{Z}$), one has

$$\alpha\big((0, N)\big) = \left| 2 \cos \frac{\pi m}{N} - 1 \right| \tag{4.8}$$

(this formula gives the correct answer $\alpha(p) = 0$ also when $N = 3m$).

(vi)

$$\lim_{|p|\to\infty} \alpha(p) = 0. \tag{4.9}$$

Proof.

(i) The claim about the maximum is straightforward, since the only maximum point $(0,0)$ of F in B belongs to B_p for any p.

(ii) The expression (3.15) shows that the set of points $\theta \in B$ where $F = 1$, consists of four lines $\theta_j = \pm\pi$, as well as two lines $\theta_1 - \theta_2 = \pm\pi$. Since no line $p \cdot \theta = 0$ can miss all these points, we conclude that $\alpha(p) \leq 1$ for any p. The inequality $\alpha(p) \geq 0$ is obvious, since, as we have already discovered, the expression under the square root in (3.15) has its minimum equal to 0.

(iii) As we have already indicated before, the points where F reaches its minimum are $(2\pi/3, -2\pi/3)$ and $(-2\pi/3, 2\pi/3)$. Thus, for $\alpha(p) = 0$ to hold, one of the lines $p \cdot \theta = 2\pi n$ must pass through one of these points. Thus, $p_1 - p_2 = \pm 3n$, and the claim is proven.

(iv) In order for $\alpha(p)$ to be equal to 1, the lines $p \cdot \theta \in 2\pi\mathbb{Z}$ should not enter the zones where $F < 1$ (shaded in Fig. 6). It is clear that when p_1, p_2 are of the same sign, this is impossible for the line $p \cdot \theta = 0$, unless one of the coordinates p_j is equal to zero. One can assume then, due to symmetries, that $p = (0, N)$, $N > 0$. In this case, the line $p \cdot \theta = N\theta_2 = 2\pi$ enters the shaded region, unless $N \leq 2$.

If the coordinates p_j have opposite signs, then in order for the first "non-trivial" line $p \cdot \theta = \pm 2\pi$ not enter the Brillouin zone (and thus in particular the shaded area), one has to satisfy the condition $|p_1\pi - p_2\pi| \leq 2\pi$. Due to the signs of p_js being opposite, this means that $|p_1| + |p_2| \leq 2$. This restricts the situation to the vectors $p = (1, -1)$ and $(-1, 1)$ only, which do satisfy $\alpha(p) = 1$. If this line does enter the Brillouin zone, the only case when the shaded area is not entered is when $p = (2, -2)$ or $(-2, 2)$ and thus the line goes along the boundary of the shaded region.

(v) In order to find $\alpha(p)$, we need to minimize F over the set of lines $p \cdot \theta = 2\pi n$ for all such integers n that the line intersects the Brillouin zone B. This entails first determining the appropriate of value of n and then minimizing over the corresponding line. The minima of F are located at the points $(-2\pi/3, 2\pi/3)$ and $(2\pi/3, -2\pi/3)$ and are the only local minima in the shaded regions shown in Fig. 6. Thus, we need to find the value of n that provides a line closest to a minimum point (see again Fig. 6). Evaluating $p \cdot \theta$ at the point $(-2\pi/3, 2\pi/3)$, we get $2\pi(p_1 - p_2)/3 = 2\pi(m \pm 1/3)$. This suggests that the line $p \cdot \theta = 2\pi m$ is the right one.

When $p = (0, N)$ with $N = 3m \pm 1 > 2$, we conclude that we need to minimize F over the line $N\theta_2 = 2\pi m$. Substituting the value $\theta_2 = 2\pi m/N$ into the modified expression for F,

$$F(\theta_1, \theta_2) = \sqrt{1 + 4\cos\frac{\theta_2}{2}\Big[(\cos\frac{\theta_2}{2} + \cos\Big(\theta_1 - \frac{\theta_2}{2}\Big)\Big]}, \tag{4.10}$$

leads to a simple minimization with respect to θ_1 and thus to the formula (4.8).

(vi) This claim is clear, since when $|p| \to \infty$, the lines $p \cdot \theta \in 2\pi\mathbb{Z}$ form a dense set in B, and thus the minimum of F over B_p approaches zero. □

Let us now concentrate for a moment on the additional pure point spectrum that arises due to the linear level sets described in Lemma 4.1. Let us assume that $p = (0, 2N)$, $N \in \mathbb{Z}$. Then, according to that lemma, the line $p \cdot \theta = 2N\pi$ is a level 1 set of $F(\theta)$. Consider λ such that $\eta(\lambda) = 1/3$ (or $\eta(\lambda) = -1/3$). We will now construct a compactly supported eigenfunction for $H_{(0,2N)}$. In order to do so, let us notice that $\eta(\lambda) = 1/3$ means that $\varphi'_{1,\lambda}(0) = 3\varphi'_{1,\lambda}(1)$. Let us construct a function φ_+ on the boldface structure Z in Fig. 7 below. It is constructed as

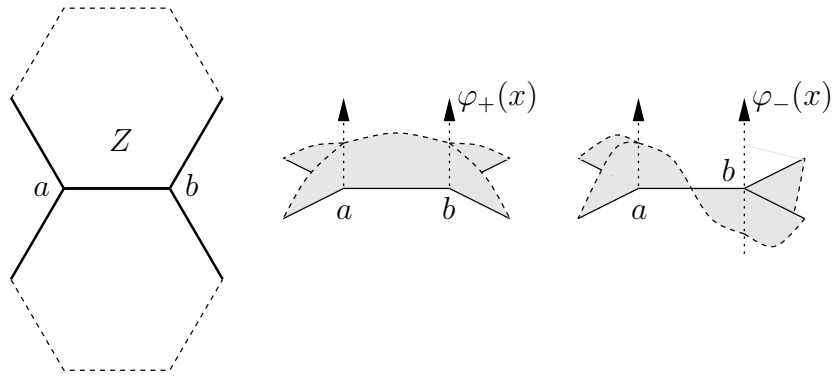

FIGURE 7. The extra eigenstates outside the Dirichlet spectrum for the zig-zag nano-tubes with even number of "zig-zags". On the left, the support is shown; on the right, the eigenfunctions $\varphi_\pm$ corresponding to the smallest solution of $\eta(\lambda) = \cos\sqrt{\lambda} = \pm 1/3$ are plotted (in the case of zero potential $q_0 = 0$).

follows: on the two "horns" directed toward the vertex a, we define the function to be equal to $\varphi_{1,\lambda}(x)$. It is similarly defined on the "horns" leading towards b. On the "bridge" between a and b, we define the function as $\varphi_{0,\lambda} + \varphi_{1,\lambda}$. It is easy to conclude that the equality $\varphi'_{1,\lambda}(0) = 3\varphi'_{1,\lambda}(1)$ implies that the function satisfies Neumann conditions at both vertices (and certainly the equation $H\varphi = \lambda\varphi$ on the edges of Z). The graph of the function φ_+ is visualized in the middle of Fig. 7.

Analogously, if $\eta(\lambda) = -1/3$, one creates a function φ_-, changing the value on the bridge to $\varphi_{0,\lambda} - \varphi_{1,\lambda}$ (see the right graph in Fig. 7).

The functions $\varphi_\pm$ are defined on Z only, but can be extended to the whole structure G as follows: one repeats the functions up and down (to dashed-line hexagons in Fig. 7), alternating the sign. Outside this column of hexagons, we define the functions to be equal to zero. These functions are periodic with respect to the vector $\vec{e}_2$ with period 2, and thus define compactly supported eigenfunctions for any even zig-zag nano-tube $T_{(0,2N)}$. We will call such eigenfunctions the *three-leaf eigenfunctions* (the name suggested by the right graph in Fig. 7).

We are now ready to establish the main result about the spectra of carbon nano-tubes. First of all, let us collect all the notions we need here. As before, $p = (p_1, p_2) \in \mathbb{Z}^2$ is a translation vector that determines the nano-tube T_p. The Hamiltonian H_p on $L_2(T_p)$ is defined as before, using the pull-back of a potential $q_0(x)$ on $[0, 1]$ symmetric with respect to the point $1/2$. We also denote by $D(\lambda)$ the Hill discriminant (trace of the monodromy matrix) of the Hill operator H^{per} on $\mathbb{R}$ with periodized potential q_0. The subset B_p of the Brillouin zone B is

defined in (4.3). Finally, the function $F(\theta)$ of the quasimomentum θ is defined in (3.15), and $\alpha(p)$ is described in Lemma 4.2.

In order to avoid lengthy formulation, in the Theorem and two Corollaries below, when dispersion relations are described, the flat branches corresponding to the pure point spectrum are omitted. The pure point spectra (and thus the flat branches) are described in separate statements.

Theorem 4.3.

(i) *The non-constant part of the dispersion relation for H_p is provided by*

$$D(\lambda) = \pm\frac{2}{3}F(\theta), \qquad \theta \in B_p. \tag{4.11}$$

(ii) *The singular continuous spectrum $\sigma_{\rm sc}(H_p)$ is empty.*

(iii) *The absolutely continuous spectrum is given by*

$$\sigma_{\rm ac}(H_p) = D^{-1}\Big(\big[-2, -\frac{2}{3}\alpha(p)\big] \cup \big[\frac{2}{3}\alpha(p), 2\big]\Big) \tag{4.12}$$

and

$$D^{-1}\Big(\big[-2, -\frac{2}{3}\big] \cup \big[\frac{2}{3}, 2\big]\Big) \subseteq \sigma_{\rm ac}(H_p) \subseteq \sigma(H^{\rm per}) = D^{-1}\big([-2, 2]\big). \tag{4.13}$$

(iv) *$\sigma_{\rm ac}(H_p) = \sigma(H^{\rm per})$ if and only if $p_1 - p_2$ is divisible by 3.*

(v) *$\sigma_{\rm ac}(H_p) = D^{-1}\big([-2, -\frac{2}{3}] \cup [\frac{2}{3}, 2]\big)$ if and only if T_p is either a $(0,1)$-, or a $(0,2)$- zig-zag nano-tube (or equivalent, e.g. $T_{(1,-1)}$).*

(vi) *Unless T_p is a zig-zag nano-tube with an even number of zig-zags (i.e., $T_{(0,2N)}$), one has*

$$\sigma_{\rm pp}(H_p) = \Sigma^{\rm D}. \tag{4.14}$$

This spectrum consists of one edge of each spectral gap (including the closed ones) of $\sigma(H^{\rm per})$. All these eigenvalues are of infinite multiplicity and the corresponding eigenspaces are spanned by simple loop eigenfunctions (supported on a single hexagon) and tube loop eigenfunctions (supported on a loop around the tube).

(vii) *If T_p is a zig-zag nano-tube with an even number of zig-zags (i.e., $T_{(0,2N)}$), one has*

$$\sigma_{\rm pp}(H_p) = \Sigma^{\rm D} \cup \Xi, \tag{4.15}$$

where

$$\Xi = D^{-1}\Big(\pm\frac{2}{3}\Big). \tag{4.16}$$

The eigenvalues from Ξ are of infinite multiplicity, are embedded into $\sigma_{\rm ac}(H_p)$, and are located two per each band of $\sigma(H^{\rm per})$. The corresponding eigenspaces are generated by the compactly supported three-leaf functions.

The eigenvalues from $\Sigma^{\rm D}$ are of infinite multiplicity and the corresponding eigenspaces are spanned by simple loop eigenfunctions and tube loop eigenfunctions.

(viii) *If $p_1 - p_2$ is divisible by 3, the ac-spectrum of H_p has exactly the same gaps as $\sigma(H^{\rm per})$. Otherwise, there is an additional gap $D^{-1}\big((-\frac{2}{3}\alpha(p), \frac{2}{3}\alpha(p))\big)$ inside each band of the spectrum of $H^{\rm per}$.*

Proof.

The first statement coincides with (4.6).

The claim (ii) is proven exactly as the corresponding statement in Theorem 3.6.

Statements (iii) through (v) follow from (i) and Lemma 4.2.

The statement (vi) is almost completely proven, except the description of the eigenfunctions. The proof of this description works exactly like in Theorem 3.6, except that the procedure of eliminating hexagons does not have to end with an empty set. One can end up with a loop of edges around the tube, which thus does not encircle any hexagons. This would provide a loop eigenfunction that runs around the tube, rather than around a hexagon. The similar claim in (vii) concerning the eigenvalues from Σ^{D} is proven exactly the same way.

What remains to be proven in (vii), is the structure of the eigenfunctions corresponding to $\lambda \in \Xi$. It is proven similarly to the structure of eigenfunctions corresponding to Σ^{D}. Indeed, again according to [35], the eigenspace is spanned by compactly supported eigenfunctions. Consider the outer boundary of the support and start eliminating hexagons inside as follows. There must be a vertex (like the ends of horns in Fig. 7) that borders zero values. Then, on the corresponding horn the function must be proportional to $\varphi_{1,\lambda}$. Let us now extend it to a three-leaf eigenfunction and subtract from the original one. Continuing this process, we eventually eliminate all hexagons. Notice that in this case we cannot end up with a loop around the tube, since this would force all the vertex values to be equal to zero, which is impossible, when λ does not belong to Σ^{D}. Thus, only the three-leaf states enter the eigenfunction.

The statement (viii) follows from the previous ones. □

We will specify this result for the cases of zig-zag ($p = (0, N)$) and armchair ($p = (N, N)$) nano-tubes. The zig-zag case was also considered in [26].

Corollary 4.4. *Let $T_{(0,N)}$ be a zig-zag nano-tube with N zig-zags.*

(i) *The non-constant part of the dispersion relation for $H_{(0,N)}$ is given by*

$$D(\lambda) = \pm\frac{2}{3}\sqrt{1 + 4\cos\frac{\pi n}{N}\Big[(\cos\frac{\pi n}{N} + \cos\Big(\theta_1 - \frac{\pi n}{N}\Big)\Big]}, \tag{4.17}$$

where $0 \le n < N$.

(ii) *The singular continuous spectrum is empty.*

(iii) *The absolutely continuous spectrum is given by*

$$\sigma_{\mathrm{ac}}(H_{(0,N)}) = D^{-1}\Big(\big[-2, -\frac{2}{3}\alpha\big] \cup \big[\frac{2}{3}\alpha, 2\big]\Big) \tag{4.18}$$

where $\alpha = \alpha((0, N)) \in [0, 1]$ is defined in (4.8). In particular, $\alpha = 0$ (i.e., $\sigma_{\mathrm{ac}}(H_{(0,N)}) = \sigma(H^{\mathrm{per}})$) if and only if N is divisible by 3. Furthermore, $\alpha = 1$ if and only if $N = 1$ or $N = 2$.

(iv) *If N is odd, then the pure point spectrum is given by $\sigma_{\mathrm{pp}}(H_{(0,N)}) = \Sigma^{\mathrm{D}}$. The corresponding eigenspaces are infinite-dimensional and generated by simple loop eigenfunctions (supported on a single hexagon) and tube loop eigenfunctions (supported on a loop around the tube).*

If N is even, then $\sigma_{\mathrm{pp}}(H_{(0,N)}) = \Sigma^{\mathrm{D}} \cup \Xi$ where Ξ is defined in (4.16). In particular, if $N = 2$ then the embedded eigenvalues from Ξ are located

at the band edges of $\sigma_{\rm ac}(H_p)$. *If* $N > 2$ *is even, this new point spectrum is located inside the bands. The eigenspaces corresponding to* Ξ *are infinite-dimensional and generated by the compactly supported three-leaf functions.*

(v) $\sigma(H_{(0,N)})$ *has additional gaps (other than the gaps of* $\sigma(H^{\rm per})$*) if and only if* N *is not divisible by* 3.

Remark 4.5. In order to avoid confusion, we need to specify what a simple loop eigenstate is for the case of the necklace tube $T_{(0,1)}$. In this case, the image of a hexagon in the tube is a "dumbbell" consisting of two beads of the necklace connected with a link (see Fig. 8 below). A simple loop eigenfunction in this case

FIGURE 8. A dumbbell image of a hexagon.

can concentrate either on a single bead, or on the whole dumbbell.

Corollary 4.6. *Let* $T_{(N,N)}$ *be an armchair nano-tube.*

(i) *The non-constant part of the dispersion relation for* $H_{(N,N)}$ *is given by*

$$D(\lambda) = \pm\frac{2}{3}\sqrt{1 + 8\cos\Big(\theta_1 - \frac{\pi n}{N}\Big)\cos\Big(\frac{\theta_1}{2}\Big)\cos\Big(\frac{\theta_1}{2} - \frac{\pi n}{N}\Big)}, \tag{4.19}$$

where $0 \le n < N$.

(ii) *The singular continuous spectrum is empty.*

(iii) *The absolutely continuous spectrum is given by*

$$\sigma_{\rm ac}(H_{(N,N)}) = D^{-1}\big([-2,2]\big) = \sigma(H^{\rm per}). \tag{4.20}$$

(iv) *The pure point spectrum is given by* $\sigma_{\rm pp}(H_{(N,N)}) = \Sigma^{\rm D}$ *and is located at an edge of each gap in* $\sigma_{\rm ac}(H_{(N,N)})$. *The eigenvalues are of infinite multiplicity and the eigenspaces are generated by simple loop eigenfunctions (either on a single hexagon or a loop around the tube).*

(v) $\sigma(H_{(N,N)})$ *has exactly the same gaps as* $\sigma(H^{\rm per})$.

5. Final remarks

- The zig-zag nano-tube case has been thoroughly studied by a different method in [26, 27]. The methods employed in this paper seem to be significantly simpler than the ones in [26, 27] and also apply to all $2D$ carbon nano-structures such as graphene and any single-wall nano-tube.

  After the paper was accepted for publication, the authors received the preprint [6], where the case of armchair nano-tubes is considered by methods analogous to the ones of [26, 27].
- Other spectral properties of the operators H and H_p, e.g. asymptotics of gaps lengths or properties of (and formulas for) the density of states can be easily derived from the explicit dispersion relations that we obtained

and the well studied properties of the Hill discriminant. As an example, we provide a theorem below that describes the smoothness of the potential in terms of the gap decay. In order to do so, we call the gaps arising as $D^{-1}([-\frac{2}{3}\alpha(p), \frac{2}{3}\alpha(p)])$ the *odd gaps* $G_{2k-1}, k = 1, 2, ...$ and the gaps of the Hill operator the *even gaps* $G_{2k}, k = 1, 2, ...$ Notice that we count the gaps even when they close (e.g., all odd gaps close for graphene and for nano-tubes with integer $(p_1 - p_2)/3$). Let also γ_k be the lengths of the gap G_k.

In the theorem below, the operator is either the graphene operator H, or the nano-tube operator H_p.

Theorem 5.1. (i) *The periodized* $1D$ *potential* q_0 *is infinitely differentiable if and only if* γ_{2k} *decays faster than any power of* k *when* $k \to \infty$.

(ii) *The periodized* $1D$ *potential* q_0 *is analytic if and only if* γ_{2k} *decays exponentially with* k.

Since the even gaps are exactly the spectral gaps for the Hill operator with the periodized q_0, this is an immediate corollary of the results of this text and known results of the same nature for the Hill operator [12, 22, 23, 40, 57]. Statements similar to this theorem can be derived as easily for other functional classes of potentials, using the corresponding results for the Hill operator in [12].

- Albeit for graphene (as well as for the nano-tubes with $p_1 - p_2$ divisible by 3) the absolutely continuous spectrum coincides with the one of the periodic Hill operator as a set, the structure of the spectrum is different, due to the appearence of the conical singularities inside of each band of the Hill spectrum.

  Such singularities can also appear when the even gaps close, but this situation is non-generic with respect to the potential q_0. However, as we discussed above, closing the odd gaps and thus appearence of conical singularities there is mandatory for any potential in the graphene case, as well for nano-tubes T_p with $p_1 - p_2$ divisible by 3.
- As we have indicated in the beginning, quantum graphs (quantum networks) have been used to model spectra of molecules at least since [51, 54]. However, the validity of such models is still under investigation, see e.g., [13, 16, 33, 46, 47, 52] and references therein.
- The graphene operator H provides also an interesting example in terms of Liouville type theorems. As it was established in [38] (see also [37] for related considerations), the Liouville theorem for periodic operators holds if and only if the Fermi surface consists of finitely many points. Albeit this normally occurs at the spectral edges only, it was indicated in [37, 38] that in principle this can happen inside the spectrum. The graphene operator provides just such an example. Namely, a direct corollary of our results and the ones of [38] is the following

Theorem 5.2. *Let H be the graphene operator. Suppose $D(\lambda) = 0$ and $n > 0$. Then the space of solutions u of the equation*

$$Hu - \lambda u = 0$$

such that

$$|u(x)| \leq C_u(1 + |x|)^n$$

is finite dimensional.

Acknowledgments

The authors express their gratitude to E. Korotyaev, K. Pankrashkin and V. Pokrovsky for information and comments. In particular, it was V. Pokrovsky, who attracted our attention to the importance of conical singularities.

The authors are also grateful to the reviewer for useful remarks.

This research of both authors was partly sponsored by the NSF through the NSF Grant DMS-0406022. The authors thank the NSF for this support. The second author was partly supported by the DFG through the Grant Po 1034/1-1. Part of this work was done during O. P. visiting Texas A&M University. The second author thanks the DFG for this support and Texas A&M University for the hospitality.

References

[1] S. Alexander, Superconductivity of networks. A percolation approach to the effects of disorder, Phys. Rev. B, 27 (1985), 1541-1557.

[2] C. Amovilli, F. Leys and N. March, Electronic energy spectrum of two-dimensional solids and a chain of C atoms from a quantum network model, Journal of Math. Chemistry, Vol. 36, No. 2, 2004.

[3] C. Amovilli, F. Leys, and N. March, *Topology, connectivity, and electronic structure of C and B cages and the corresponding nanotubes*, J. Chem. Inf. Comput. Sci. **44** (2004), 122–135.

[4] N. W. Ashcroft and N. D.Mermin, *Solid State Physics*, Holt, Rinehart and Winston, New York-London, 1976.

[5] J. Avron, A. Raveh, and B. Zur, Adiabatic quantum transport in multiply connected systems, Rev. Mod. Phys. 60 (1988), no.4, 873-915.

[6] A. Badanin, J. Brüning, E. Korotyaev, I. Lobanov, Schrödinger operators on armchair nanotubes, preprint, (Dec 27th 2006).

[7] G. Berkolaiko, R. Carlson, S. Fulling, and P. Kuchment (Editors), *Quantum Graphs and Their Applications*, Contemp. Math., v. 415, American Math. Society, Providence, RI 2006.

[8] C. Cattaneo, The spectrum of the continuous Laplacian on a graph, Monatsh. Math. 124 (1997), no. 3, 215–235.

[9] F. Chung, *Spectral Graph Theory*, Amer. Math. Soc., Providence R.I., 1997.

[10] Y. Colin de Verdière, *Spectres De Graphes*, Societe Mathematique De France, 1998

[11] P.-G. de Gennes, Champ critique d'une boucle supraconductrice ramefiee, C. R. Acad. Sc. Paris 292B (1981), 279-282.

[12] P. Djakov and B. S. Mityagin, Instability zones of periodic 1-dimensional Schrödinger and Dirac operators, Russian Mathematical Surveys **61** (2006), no. 4, 663-766.

[13] P. Duclos, P. Exner, Curvature-induced bound states in quantum waveguides in two and three dimensions, Rev. Math. Phys. 7 (1995), 73-102

[14] P. Exner, Contact interactions on graph superlattices, J. Phys. A29 (1996), 87-102

[15] P. Exner, R. Gawlista, Band spectra of rectangular graph superlattices, Phys. Rev. B53 (1996), 7275-7286

[16] P. Exner, P. Seba, Electrons in semiconductor microstructures: a challenge to operator theorists, in Proceedings of the Workshop on Schrödinger Operators, Standard and Nonstandard (Dubna 1988), World Scientific, Singapore 1989; pp. 79-100.
[17] M. S. P. Eastham, *The Spectral Theory of Periodic Differential Equations*, Scottish Acad. Press Ltd., Edinburgh-London, 1973.
[18] J. Garnett and E. Trubowitz, Gaps and bands of one-dimensional periodic Schrödinger operators, Comment. Math. Helv. **59** (1984), no. 2, 258–312.
[19] J. Garnett and E. Trubowitz, Gaps and bands of one dimensional periodic Schrödinger operators II, Comment. Math. Helv. **62** (1987), 18–37.
[20] C. Gerard and F. Nier, The Mourre theory for analytically fibered operators, J. Funct. Anal. **152** (1998), no.1, 202-219.
[21] P. Harris, *Carbon Nano-tubes and Related Structures*, Cambridge University Press 2002.
[22] H. Hochstadt, Estimates on the stability intervals for the Hill's equation, Proc. AMS **14** (1963), 930–932.
[23] H. Hochstadt, On the determination of a Hill's equation from its spectrum, Arch. Rational Mech. Anal. **19** (1965), 353–362.
[24] V.A. Iakubovich and V.M. Starzhinski, *Linear Differential Equations with Periodic Coefficients*, Wiley, NY 1975.
[25] M. I. Katsnelson, Graphene: carbon in two dimensions, preprint arXiv:cond-mat/0612534v1 (Dec 20th 2006).
[26] E Korotyaev and I. Lobanov, Schrödinger operators on zigzag graphs, preprint arXiv:math.SP/0604006
[27] E Korotyaev and I. Lobanov, Zigzag periodic nanotube in magnetic field, preprint arXiv:math.SP/0604007
[28] V. Kostrykin and R. Schrader, Kirchhoff's rule for quantum wires, J. Phys. A 32 (1999), 595-630.
[29] T. Kottos and U. Smilansky, Quantum chaos on graphs, Phys. Rev. Lett. 79 (1997), 4794–4797.
[30] P. Kuchment, To the Floquet theory of periodic difference equations, in *Geometrical and Algebraical Aspects in Several Complex Variables*, Cetraro (Italy), June 1989, 203-209, EditEl, 1991.
[31] P. Kuchment, *Floquet Theory for Partial Differential Equations*, Birkhäuser Verlag, Basel, 1993.
[32] P. Kuchment (Editor), Quantum graphs and their applications, a special issue of Waves in Random media, 14 (2004), no.1.
[33] P. Kuchment, Graph models of wave propagation in thin structures, Waves in Random Media 12 (2002), no. 4, R1-R24.
[34] P. Kuchment, Quantum graphs: I. Some basic structures, Waves Random Media **14** (2004), S107–S128.
[35] P. Kuchment, Quantum graphs. II. Some spectral properties of quantum and combinatorial graphs, J. Phys. A **38** (2005), no. 22, 4887–4900.
[36] P. Kuchment and L. Kunyansky, Spectral Properties of High Contrast Band-Gap Materials and Operators on Graphs, Experimental Mathematics, 8 (1999), no.1, 1-28.
[37] P Kuchment and Y. Pinchover, Integral representations and Liouville theorems for solutions of periodic elliptic equations, J. Funct. Anal. 181(2001), 402–446.
[38] P Kuchment and Y. Pinchover, Liouville theorems and spectral edge behavior on abelian coverings of compact manifolds, arXiv:math-ph/0503010, to appear in Trans. Amer. Math. Soc.
[39] P. Kuchment and B. Vainberg, On the structure of eigenfunctions corresponding to embedded eigenvalues of locally perturbed periodic graph operators, Comm. Math. Phys. **268** (2006), 673-686.

[40] V. F. Lazutkin and T. F. Pankratova, Asymptotics of the width of gaps in the spectrum of the Sturm-Liouville operators with periodic potential, Soviet Math. Dokl. Vol. **15** (1974), 649–653.
[41] W. Magnus and S. Winkler, *Hill's Equation*, Wiley, NY 1966.
[42] V. A. Marchenko and I. V. Ostrovskii, A characterization of the spectrum of Hill's operator, Matem. Sborn. **97** (1975), 540–606; English transl. in Math. USSR-Sb. **26** (1975), 493–554.
[43] V. A. Marchenko and I. V. Ostrovskii, Approximation of periodic potentials by finite zone potentials. (Russian) Vestnik Kharkov. Gos. Univ. No. 205 (1980), 4–40, 139.
[44] H. P. McKean and E. Trubowitz, Hill's surfaces and their theta functions, Bull. Amer. Math. Soc. **84** (1978), no. 6, 1042–1085.
[45] R. G. J. Mills and E. W. Montroll, Quantum theory on a network. II. A solvable model which may have several bound states per node point, J. Math. Phys. 11 (1970), no. 8, 2525–2538.
[46] S. Molchanov and B. Vainberg, Transition from a network of thin fibers to the quantum graph: an explicitly solvable model, Contemporary Mathematics, v. 415, AMS (2006), pp 227-240.
[47] S. Molchanov and B. Vainberg, Scattering solutions in a network of thin fibers: small diameter asymptotics, preprint arXiv:math-ph/0609021.
[48] E. Montroll, Quantum theory on a network. I. A solwable model whose wavefunctions are elementary functions, J. Math. Phys. 11 (1970), no. 2, 635–648.
[49] V. L. Oleinik, B. S. Pavlov, and N. V. Sibirev, Analysis of the dispersion equation for the Schrödinger operator on periodic metric graphs, Waves in Random Media **14** (2004), 157–183.
[50] K. Pankrashkin, Spectra of Schrödinger operators on equilateral quantum graphs, Lett. Math. Phys. 77 (2006) 139–154.
[51] L. Pauling, The diamagnetic anisotropy of aromatic molecules, J. Chem. Phys. 4 (1936), 673–677.
[52] O. Post, Branched quantum wave guides with Dirichlet boundary conditions: the decoupling case, J. Phys. A 38 (2005), no. 22, 4917–4931.
[53] M. Reed and B. Simon, *Methods of modern mathematical physics IV: Analysis of operators*, Academic Press, New York, 1978.
[54] K. Ruedenberg and C. W. Scherr, Free-electron network model for conjugated systems. I. Theory, J. Chem. Physics, 21 (1953), no.9, 1565-1581.
[55] R. Saito, G. Dresselhaus and M.S. Dresselhaus, *Physical Properties of Carbon Nanotubes*, Imperial College Press, London, 1998.
[56] L. E. Thomas, Time dependent approach to scattering from impurities in a crystal, Comm. Math. Phys. 33 (1973), 335-343.
[57] E. Trubowitz, The inverse problem for periodic potentials, Comm. Pure and Appl. Math. **30** (1977), 321–342.
[58] V. E. Zakharov, S. V. Manakov, S. P. Novikov, L. P. Pitaevskii, *Theory of Solitons: The Inverse Scattering Method*, Plenum 1984.

Mathematics Department, Texas A&M University College Station, TX 77843-3368 USA
E-mail address: kuchment@math.tamu.edu

Institut für Mathematik, Humboldt-Universität zu Berlin, Rudower Chaussee 25, 12489 Berlin, Germany
E-mail address: post@math.hu-berlin.de